ARCHIVES OF TRANSPORT *ISSN (print):* *0866-9546*
Volume 78, Issue 2, 2026 ***e-ISSN (online):*** *2300-8830*
DOI: *10.61089/aot2026.rjmjxj94*

DESIGN OF AN INTELLIGENT INTERCOOLER CONTROL SYSTEM (IICS) FOR MITIGATING PERFORMANCE LOSS AND EMISSION IMPACT IN LPG ENGINES AT ELEVATED AMBIENT TEMPERATURES

Suroto MUNAHAR[1,2], Retno RUSDJIJATI[3], Muhtar HANAFI[4], Ari WARYONO[5], Sidqi MUBAROK[6], Muhammad Azhar ALKHADAFI[7], Moehamad AMAN[8]

[1] Center of Energy for Society and Industry (CESI), Universitas Muhammadiyah Magelang, Magelang, Indonesia
[2] Automotive Mechanical Engineering, Universitas Muhammadiyah Magelang, Magelang, Jawa Tengah, Indonesia
[3, 8] Industrial Engineering, Universitas Muhammadiyah Magelang, Magelang, Jawa Tengah, Indonesia
[4] Informatics Engineering, Universitas Muhammadiyah Magelang, Magelang, Jawa Tengah, Indonesia
[5, 6, 7] Automotive Mechanical Engineering Laboratory, Universitas Muhammadiyah Magelang, Mertoyudan, Magelang, Jawa Tengah, Indonesia

Abstract:

The increasing demand for environmentally friendly vehicles with optimal engine performance has encouraged the development of cleaner and more efficient alternative fuels, such as Liquefied Petroleum Gas (LPG). LPG has a high octane rating and is suitable for engines operating at high compression ratios. Its use also produces a self-refrigeration effect during depressurization, as the phase transition from liquid to gas absorbs heat. This cooling potential is generally dissipated into the environment, although it can be utilized to reduce intake-air temperature, which is particularly important for maintaining volumetric efficiency and engine power under high ambient temperatures. Therefore, this study developed an Adaptive Intercooler Control System (AICS) that utilizes the LPG self-refrigeration effect as a cooling medium for engine intake air. The AICS was experimentally evaluated on a 135cc engine based on engine performance, heat transfer characteristics, and exhaust emissions. The results showed that AICS operation increased engine power by approximately 0.7–1.0 HP (13–18%) at 4800–5200 rpm and increased torque by 0.2–0.4 Nm at 4000–5000 rpm. At idle speed, the system reduced HC emissions from 1020 to 890 ppm and CO emissions from 5.3% to 4.8%. Thermally, AICS optimized heat transfer within the intercooler, achieving an air-side heat transfer rate of approximately 5.5–5.6 W over 25–35 s. The LPG-side heat transfer rate remained stable at approximately 20–26 W throughout the testing period. These findings demonstrate that controlled utilization of LPG self-refrigeration through AICS can improve intake-air thermal management, enhance engine performance, and reduce exhaust emissions.

Keywords: *Intelligent Intercooler Control System (IICS), LPG, self-refrigeration effect, emissions, engine power*

To cite this article:

Munahar, S., Rusdjijati, R., Hanafi, M., Waryono, A., Mubarok, S., Alkhadafi, M.A., Aman, M. (2026). Design of an Intelligent Intercooler Control System (IICS) for mitigating performance loss and emission impact in LPG engines at elevated ambient temperatures. Archives of Transport, 78(2), 145-170. https://doi.org/10.61089/aot2026.rjmjxj94

Contact:
1) munahar@unimma.ac.id [https://orcid.org/0000-0002-8236-0741] - corresponding author; 2) rusdjijati@ummgl.ac.id [https://orcid.org/0000-0002-3771-5857]; 3) hanafi@unimma.ac.id [https://orcid.org/0000-0003-0670-3359]; 4) ariwaryono9@gmail.com [https://orcid.org/0009-0007-9218-6752]; 5) mubarak_81@gmail.com [https://orcid.org/0009-0001-6502-0833]; 6) Azhar@gmail.com [https://orcid.org/0009-0004-4120-2028]; 7) aman@unimma.ac.id [https://orcid.org/0009-0002-7033-5167];

Article is available in open access and licensed under a Creative Commons Attribution 4.0 International (CC BY 4.0)

1. Introduction

Energy demand in the transportation sector is increasing significantly at both global and regional scales, with fossil fuels accounting for the larger proportion. The increasing consumption of fossil-based energy has contributed to adverse impacts on human respiratory health and environmental degradation (Mahlangeni et al., 2025; Wallbanks et al., 2024). Additionally, the extensive use of fossil fuels has accelerated global climate warming, triggered extreme weather changes, and contributed to sea level rise (Bergougui, 2024). These conditions show the growing importance of adopting alternative energy sources, such as Liquefied Petroleum Gas (LPG), that are environmentally friendly, sustainable, and economically viable to support the development of greener transportation systems (Anantama et al. 2023; KOZYRA et al. 202; Vishnuram et al. 2025).

LPG is currently considered a promising alternative energy source for use as a fuel in the transportation sector. The widespread use of LPG as a vehicle fuel is supported by several factors, including relatively stable availability, an established distribution network in many countries, and lower operational costs compared to conventional fuels. Additionally, LPG possesses a relatively high energy content, an elevated octane rating, and produces lower emissions, showing potential as a feasible fuel for vehicle applications (Churchill et al., 2025; Dafis et al., 2026; Matthujak et al., 2021). The lower operating pressure compared to other gaseous fuels also provides advantages in terms of operational safety. However, the application of LPG as a vehicle fuel still faces several limitations, particularly related to engine performance. Several studies have reported a reduction in engine power when gasoline is replaced with LPG. Simsek and Uslu (Simsek & Uslu, 2024) reported that internal combustion engines using LPG had a negative impact on power reduction but a positive impact on emission quality. This reduction in engine performance is attributed to the lower flame propagation speed compared with fossil fuels. To address the limitations, adjustments to ignition timing, compression pressure, and Air-Fuel Ratio (AFR) have been proven effective to mitigate the reduction in engine power.

Several previous studies have evaluated the performance of LPG-fueled engines by considering various operational parameters. Some of these studies have focused on volumetric efficiency analysis, exhaust emission characteristics, ignition timing control, fuel mixer design, and natural cooling phenomena attributed to the phase change of LPG. Research conducted by Talib, Al-dawody, and Sarris (Talib Hashem et al., 2023) reported that gasoline-powered engines showed higher volumetric efficiency than LPG. Another study by Masi, Massimo, and Paolo Gobbato (Masi & Gobbato, 2012) attempted to observe the volumetric efficiency characteristics of vehicles using gasoline, LNG, CNG, and LPG. However, the direct relationship between volumetric efficiency and engine power output in LPG fuel systems has not been extensively discussed in the existing literature. From an emissions perspective, the majority of studies have examined changes in exhaust gas composition in LPG-fueled engines. Usman *et al.*, (2020) investigated the emissions produced by LPG engine, focusing on carbon dioxide (CO_2), hydrocarbons (HC), and carbon monoxide (CO). Meanwhile. Meanwhile, Park and Sungwook Park (2025) and Kim et al (2025) conducted a study simulating engine power measured using a dynamometer test (dyno test) in relation to the nitrogen oxides (NOx) emissions produced. Although extensive investigations have been conducted on emissions, the relationship between ambient air temperature conditions and power reduction in LPG engine has not received sufficient attention.

In addition to combustion parameters, LPG-air mixture has been investigated to improve engine performance and emission characteristics. A previous study by Setiyo et al. (2016) and Wang et al.(2022) designed fixed mixers to improve the homogeneity of LPG-air mixture. The designed system was experimentally tested on a 1500 cc vehicle, and the power output was validated using a dynamometer test (dyno test). Mohsen *et al.*(2023) introduced compression pressure as an additional variable to evaluate the generated engine power. Meanwhile, other studies conducted by Zhang, et al.,(2022) and by Xiangyang et al (2024) investigated exhaust emission characteristics through adjustments of the spark advance system. Although studies on fuel–air mixer parameters have been conducted, there is no report addressing the self-refrigeration effect and LPG mixer in relation to changes in engine power.

As a vehicle fuel, LPG undergoes several thermodynamic transformations that generate a potentially useful cooling effect. The fuel is safely stored in a

tank under high pressure in liquid form and converted into a gaseous phase under lower pressure conditions to meet engine requirements. This liquid-to-gas phase transition absorbs heat from the surroundings, producing a self-refrigeration effect that is typically dissipated freely into the environment. Several studies have investigated the phenomenon, particularly the potential of LPG as an alternative cooling system. Leigh et at (Salamanca et al., 2024) developed LPG as a coolant in refrigerators, which produced a fairly good coefficient of performance (COP) and successfully achieved temperatures below 0°C. Meanwhile, other researchers Setiyo *et al.*, (2017a) and Setiyo *et al.*, (2017b) reported the potential of LPG as a refrigeration system based on a half-cycle process. Waluyo *et al.*, (2022) further developed the application of LPG as a cabin cooling system in vehicles. Despite the numerous reports, there is no information on the use of heat absorption capability of LPG as a cooling system to enhance engine performance.

The potential of the cooling effect is particularly relevant to internal combustion engines, where performance is strongly influenced by the volumetric efficiency of the intake air. Under high ambient temperature conditions, the volumetric efficiency decreases, which reduces the generated engine power (Hofmann, 2017). At low temperatures, operational disturbances may occur, particularly during the air–fuel mixing process and engine cold starts. Several studies have reported an ideal operating temperature of approximately 20–30°C (Amer et al., 2015; Salman et al., 2020).

Previous studies on LPG engines have been conducted using various variables, including emission characteristics, volumetric efficiency, fuel–air mixing system design, and engine parameter optimization. However, several important aspects remain insufficiently explored, particularly the development of a control system designed to prevent engine power loss caused by reduced volumetric efficiency during high ambient temperatures by leveraging the self-cooling effect in LPG engines. Intercoolers have been applied to internal combustion engines specifically diesel engines as discussed by (Cipollone et al., 2017) and (Novella et al., 2017). However, a drawback of this system is that it requires energy to operate, thereby reducing the power generated by the engine. In contrast, the research conducted here utilizes exhaust energy, thereby avoiding any reduction in engine power. Therefore, this study proposes a novel approach through the development of an Adaptive Intercooler Control System (AICS) designed to cool the intake air entering the engine. The proposed system aims to reduce engine power losses and decrease exhaust emissions while simultaneously enhancing engine power output through improved volumetric efficiency by utilizing the LPG self-refrigeration effect, which has rarely been investigated in previous studies. The novelty of this research lies in the design of AICS, which is able to control the intake air cooling process based on the self-cooling effect of the LPG engine to prevent engine power loss at high ambient temperatures. To date, the LPG self-refrigeration effect has generally been released directly into the surrounding environment without being utilized as a potential method for improving engine performance. This study extends previous activities that were developed only on a mathematical model scale with MATLAB Simulink by implementing the proposed concept in real vehicles (Munahar et al., 2026).

2. Methods

2.1. Set up Research Apparatus

In designing AICS, several stages were carried out systematically. The initial stage started with the development of the installation scheme for AICS components, as shown in Figure 1. The control system consisted of, namely (1) LPG tank, (2) shut-off valve, (3) weight scale, (4) expansion valve, (5) evaporator/intercooler, (6) converter kit, (7) mixer, (8) throttle body, (9) engine, (10) Electronic Control Module (ECM), (11) main solenoid, (12) bypass solenoid, and (13) Exhaust Gas Analyzer (EGA). Engine power performance testing was conducted using a dynamometer, with the throttle fully open and a single driver in the vehicle (14). Subsequently, heat transfer characteristics of LPG and air were measured using data acquisition. LPG emissions and AFR were measured using Exhaust Gas Analysis (EGA) meter. A weight scale and time-varying measurements were used to determine LPG flow rate. A temperature sensor (T4) was used to measure the air entering the intake manifold. The air entering the intercooler was measured using a temperature sensor (T5). LPG entering and leaving the intercooler was determined using sensors T(3) and T(2) for LPG temperature changes. Heat transfer characteristics of LPG and air were measured using a data

acquisition system. LPG emissions and AFR were evaluated using EGA meter and AFR meter. LPG mass flow rate was determined using a balance combined with time-varying measurements. T4 sensor was used to measure the temperature of the air entering the intake manifold, while T5 was used for air entering the intercooler. Furthermore, the inlet and outlet temperatures of LPG flowing through the intercooler were measured using temperature sensors T3 and T2, respectively, to capture LPG temperature variations during heat transfer process.

In order to ensure adequate experimental conditions, several parameters were kept constant and some parameters were varied. The parameters kept constant include: 1) The vehicle load is carried by a person weighing approximately 65 kg. 2) The engine ignition timing is set at 5◦ before TDC (Top Dead Center). 3) The test vehicle uses a vehicle of the same type. Meanwhile, the parameters varied include: 1) The temperature of the air entering the engine is varied using a heater. 2) The vehicle engine is operated in the range of 4000-6500 rpm.

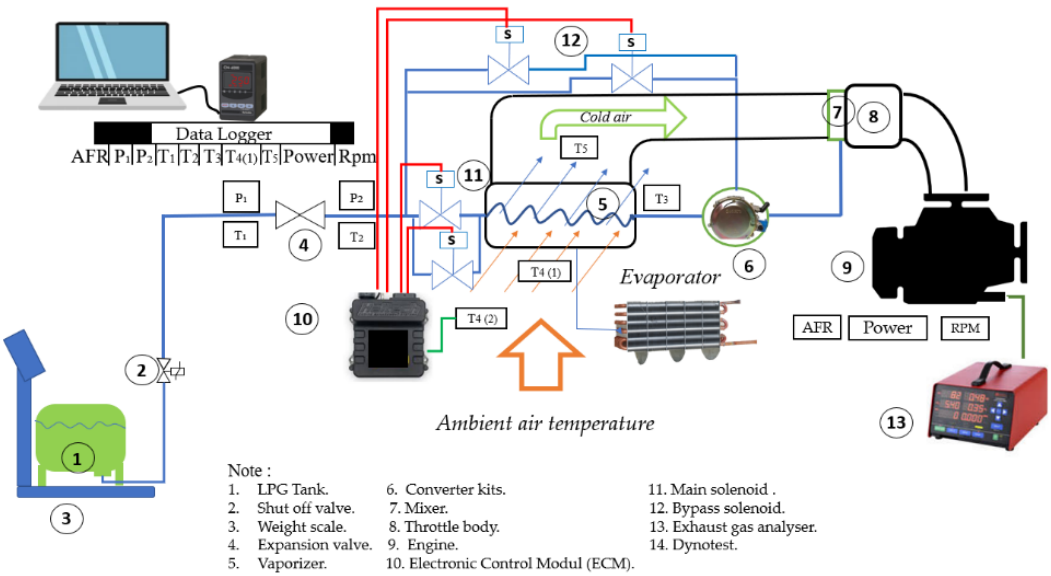



Fig. 1. Settings of AICS

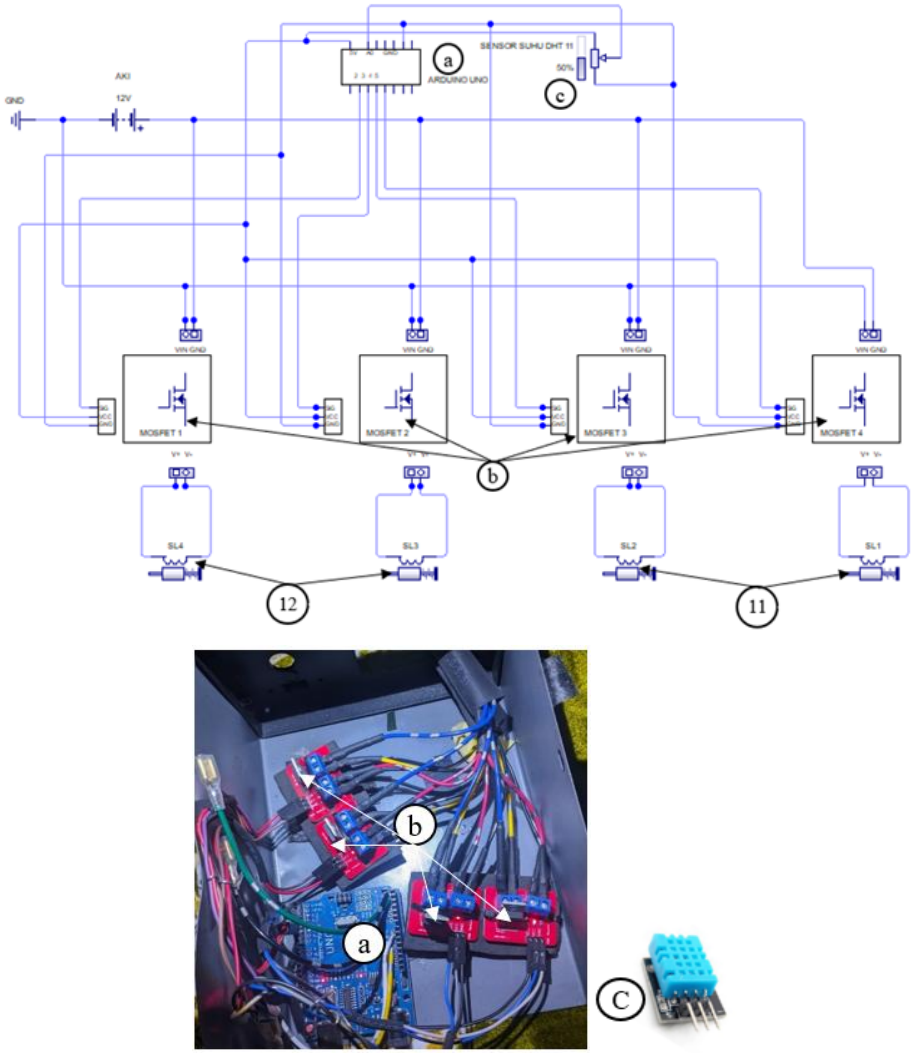

Fig. 2. ECU wiring diagram.

The designed ECM has a wiring diagram consisting of several components, as shown in Figure 2. ECM is an integrated circuit system composed of (a) AT-Mega microcontroller, (b) MOSFET, and (c) air temperature sensor. Meanwhile, components (11) the main solenoid and (12) the bypass solenoid were used to regulate LPG flow and were installed near the engine. The developed control system was implemented using a microcontroller programmed in the C programming language, as presented in the Appendix.

2.2. Equipment Specifications

The equipment used in this study consisted of several components, including a motorcycle, a microcontroller, and solenoid valves, with their specifications presented in Table 1.

Table 1. The equipment specifications.

No.	Description	Specification	Information
1.	Motorcycle	Yamaha	Test vehicle
2.	Engine Volume	135 cc	
3.	Engine Type	4 strokes	
4.	Transmission	5 speeds	
5.	Rear Brake	Brake drum	
6.	Front Brake	Disc brake	
7.	Microcontroller Type	ATmega 328P	Microcontroller for ECU controller
8.	Speed Clock	16 MHz	
9.	Flash Memory	32 KB	
10.	Analog Input Pins	6 Pins	
11.	EEPROM	1 KB	
12.	Voltage	12 Volt	Solenoid
13.	LPG working pressure	1 -12 bar	Fuel tank
14.	MOFSET	IRF 520	Solenoid control module
15.	Solenoid	12 Volt	Main and Bypass
16.	Air temperature sensor	DH11	Measuring range 0 – 60^{0}C with humidity 20-90%.
17.	Evaporator	Dimensions of 15 x 10 x 10 cm with a front area of 12 x 7 cm = 105 cm²	Cross-sectional area for heat transfer: 3,935.51cm^2

2.3. Effect of LPG Self-Refrigeration

The self-refrigeration effect in LPG is a thermodynamic phenomenon caused by a sudden pressure reduction that induces flash evaporation in a portion of the fluid. This phenomenon leads to heat absorption from the surrounding environment, thereby producing a cooling effect. The magnitude of the effect is generally influenced by the thermodynamic characteristics of the gas. LPG is a hydrocarbon mixture, primarily consisting of propane and butane, which is stored under high-pressure conditions to maintain the liquid phase. In engine fuel applications, LPG must undergo a pressure reduction to meet combustion requirements. This process causes a phase change that generates a self-refrigeration effect. However, the cooling effect has not been utilized optimally and is often released directly into the environment without thermal energy recovery. This limits its potential benefits of LPG-based cooling for improving engine performance and thermal management.

2.4. Adaptive Intercooler Control System (AICS)

AICS is an innovation in thermal management for LPG-fueled engines. This system is designed to operate adaptively to enhance engine performance, particularly under conditions of elevated ambient temperatures caused by high solar radiation or urban environments with significant heat loads. AICS method uses temperature sensors and ECM to monitor and regulate the cooling process in real time based on engine operating conditions. Adaptive control of the solenoid valves and regulation of LPG flow enable optimization of engine performance under high thermal load conditions. The implementation of this system, including the specifications of ECM used, contributes to improved engine power output, reduced emissions, and the recovery of thermal energy that will be dissipated into the environment.

2.5. Control System Algorithm

The control system algorithm developed in this study described the mechanism for regulating LPG flow entering the engine, as shown in Figure 3. The system started with the measurement of intake air temperature through the intake manifold, which is converted into digital data. The microcontroller, as part of ECM, was used to determine the control action based on a comparison between the measured temperature and a predefined threshold value. The initial stage started with a sensor measuring the intake air temperature through the intake manifold. The sensor output, which was initially in analog form, was converted using Analog-to-Digital Converter (ADC) into digital data that could be processed by ECM. Subsequently, ECM compared the

temperature value with a threshold of 30°C. When the intake air temperature is greater than 30°C (T > 30°C), the system operates under condition S1. However, when the intake air temperature is lower than 30°C (T < 30°C), the system operates under condition S2.

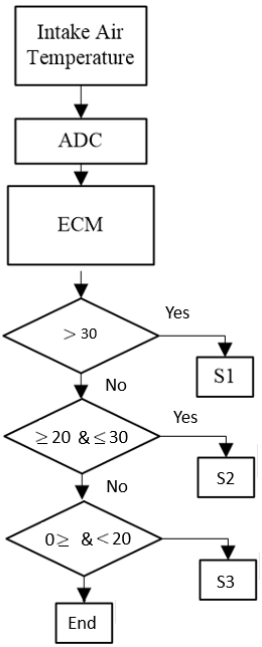

Fig. 3. Control system algorithm

The ambient air conditions in this study are classified into three states S1, S2, and S3 as presented in Table 2. Condition S1 represents a high ambient temperature state, which has the potential to reduce LPG engine performance due to the rise in intake air temperature. Under this condition, an intake air cooling system is required to reduce the spacing between air molecules, thereby improving combustion quality and optimizing engine power output. To achieve this, both main solenoids are activated (On) and both bypass solenoids are deactivated (Off), allowing LPG in the gas phase to flow through the intercooler; this provides a natural cooling effect by absorbing heat from the intake air flowing toward the engine.

In comparison, condition S2 represents a state of relatively low ambient temperature, where intake air cooling is less necessary. Under this condition, one main solenoid and the bypass solenoid are deactivated (Off) to prevent the LPG from cooling the intake air.

Condition S3 represents the lowest ambient temperature state, where intake air cooling is no longer required. Under this condition, both main solenoids are deactivated (Off) and the bypass solenoids are activated (On) to prevent the LPG from cooling the intake air. Such temperatures can trigger condensation (dew point formation), potentially disrupting the combustion process within the engine. However, condition S3 is not reported in this article; the study focuses on the implementation of conditions S1 and S2, as these sufficiently demonstrate the impact of using an intercooler on changes in power and torque.

Table 2. Status of conditions S1, S2 and S3.

Status	Main solenoid		By pass solenoid	
	1	2	1	2
S1	On	On	Off	Off
S2	On	Off	On	Off
S3	Off	Off	On	On

2.6. Analysis of Heat Transfer in Intercooler

Analysis of heat transfer in the intercooler was conducted using several mathematical equations. The initial stage included determining LPG mass flow rate ($\dot{m}_{LPG}$), which was obtained through measurements using a digital scale. The scale was used to measure the change in LPG mass consumed over a specific time interval, as expressed in Equation (1). Subsequently, LPG mass flow rate (g/s) was calculated based on the difference between the initial mass (m_1) and the final mass (m_2), divided by the measurement duration (t). The air mass flow rate ($\dot{m}_{air}$) entering the engine was determined using Equations (2) and (3). This value was obtained from the product of AFR and LPG mass flow rate ($\dot{m}_{LPG}$). AFR, representing the proportion of air to fuel, was measured using AFR meter/EGA installed in the exhaust system. AFR value was determined using Equation (1).

$$AFR = \frac{\dot{m_{air}}}{\dot{m_{LPG}}} \tag{1}$$

$$\dot{m}_{LPG} = \frac{m_1 - m_2}{t} \tag{2}$$

$$\dot{m_{air}} = AFR \times \dot{m_{LPG}} \quad (3)$$

After obtaining AFR value, LPG and air flow rates were subsequently used to calculate LPG heat transfer rate in the intercooler. The magnitude of LPG heat transfer rate was calculated using Equation (4), expressed as (q_{lpg}). This heat transfer was determined from the product of the enthalpy change (ΔH) and LPG (Setiyo et al., 2022)(Ohunakin et al., 2017). The enthalpy change of LPG is calculated using Equation (5), which is based on the difference between the fluid enthalpy at the inlet and outlet conditions of the intercooler. LPG enthalpy value (ΔH) is associated with the difference in thermodynamic conditions before and after heat transfer process in the intercooler. The enthalpy data used in this study were obtained from the thermodynamic properties of LPG, consisting of a 50% propane–butane mixture. These values were determined based on the fluid conditions at the inlet and outlet sides of the intercooler, thereby representing the energy changes occurring during the cooling process.

$$q_{LPG} = \dot{m_{LPG}} \times \Delta h \quad (4)$$

$$\Delta H = 0{,}5(propana + butana)_1 - 0{,}5\ (propana + butana)_2 \quad (5)$$

Heat transfer rate was calculated using Equation (6), while the air flow rate was determined using Equation (5) by multiplying AFR by LPG flow rate under each test condition. The specific heat capacity of air was assumed to be constant at 1,140 J·kg^{-1}·°C^{-1} for a temperature of 40°C and relative humidity of approximately 90% (Sammour et al. 2023). The air mass flow rate $\dot{m}_{air}$ within the intercooler is expressed in kg.s^{-1}. Meanwhile, ΔT_{air} represents the temperature difference of the air passing through the intercooler, expressed in °C. The temperature difference data for both air and LPG were collected using a real-time data acquisition system installed on the test vehicle.

$$q_{air} = \dot{m_{air}} \times CP_{air} \times \Delta T_{air} \quad (6)$$

2.7. Statistical Analysis for Testing Engine Performance Data

The engine power and torque data obtained from LPG-fueled engine tests were statistically analyzed to verify the reliability of the measurement results. Statistical analysis was performed using the non-parametric Wilcoxon Signed-Rank Test, which was considered appropriate for analyzing two related samples. The reliability of the measurement results was evaluated at a 95% confidence level with a significance level (α) of 0.05. The statistical analysis of the engine power and torque data was carried out using IBM SPSS Statistics. For this analysis, two hypotheses were formulated, including the null hypothesis (H_0) and the alternative hypothesis (H_1). The null hypothesis (H_0) stated that the implementation of AICS had no statistically significant effect on improving engine power and torque. Meanwhile, the alternative hypothesis (H_1) stated that the implementation of AICS had a statistically significant effect on improving engine power and torque. The hypothesis testing results were interpreted based on the *p*-value obtained from the SPSS analysis. When the *p*-value was less than or equal to 0.05, the null hypothesis (H_0) was rejected in favor of the alternative hypothesis (H_1). However, when the *p*-value was greater than 0.05, the null hypothesis (H_0) was not rejected.

Furthermore, descriptive statistics were used to analyse changes in AFR, LPG flow rate, airflow rate, the temperature difference of air passing through the intercooler, the LPG temperature difference, air heat transfer, and LPG heat transfer. The analysis utilized Standard Deviation (SD) and Margin of Error (MoE), as presented in Equations (7) and (8). SD and MoE were employed to analyse the AICS once the data had stabilized; this condition occurred between the 20-second and 100-second marks, comprising a total of 80 data points. Where x is the observed data, Z is the confidence level, and n is the number of data points or samples.

$$SD = \sqrt{\frac{\sum_{i=1}^{n}(xi - \bar{x})}{n-1}} \quad (7)$$

$$MoE = Z \times \frac{SD}{\sqrt{n}} \quad (8)$$

3. Result and Discussion

3.1. Changes in LPG Engine Emission Values with AICS

LPG engine emission measurements were carried out at idle speed (approximately 1,000 rpm), no load, and closed throttle valve which is presented in

Figure 4. Because the measurement is carried out at idle engine conditions, the measurement method has uncertainty when the vehicle is measured at engine speeds, engine loads and throttle valve openings that vary.This Figure 4 informs about the changes in exhaust emissions with and without the Adaptive Intercooler Control System (AICS). This figure provides information regarding the comparison of LPG engine exhaust emission characteristics analyzed through five main parameters: HC, CO, AFR, CO_2, and O_2. For the hydrocarbon (HC) parameter, the emission value decreased significantly from approximately 1020 ppm (without AICS) to 890 ppm (with AICS). In terms of carbon monoxide (CO), a significant reduction was observed from approximately 5.3% to 4.8% when AICS was applied. This reduction indicated that the combustion process became more complete, as CO was a primary indicator of incomplete combustion. With the implementation of AICS, the intake air temperature decreased, leading to higher air density, which improved the air–fuel mixing ratio.

AFR value showed a slight increase from 14.75 (without AICS) to 14.85 (with AICS), reaching the stoichiometric condition. This increase indicated that the mixture became leaner (containing more air), which contributed to better combustion efficiency and lower CO emissions. For carbon dioxide (CO_2) emissions, an increase was observed from approximately 4.8% to 5.2% with the use of AICS. The increase in CO_2 was considered a positive indication that combustion occurred more completely, as more carbon was fully oxidized into CO_2 rather than CO. Meanwhile, the oxygen (O_2) content in the exhaust gas increased from approximately 4.5% to 6.3%. This result indicated the presence of excess air during the combustion process, which was consistent with the increase in AFR. The excess O_2 also contributed to suppressing CO formation.

The implementation of AICS was proven to improve the combustion quality of LPG engine through an increase in intake air density. This improvement produced lower CO emissions, higher CO_2 emissions, as well as enhanced AFR and O_2 content. Therefore, the intercooler played a major role in thermal management, providing a significant contribution to emission reduction and the improvement of combustion system efficiency.

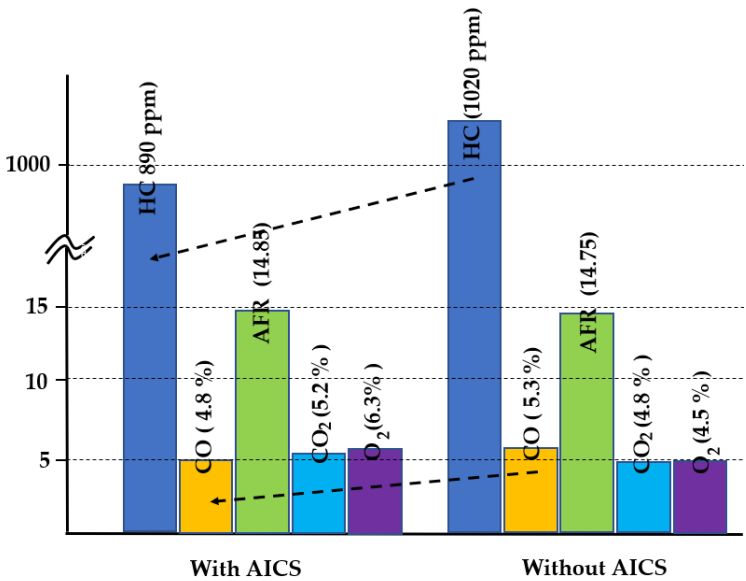

Fig. 4. Changes in LPG engine emission reduction

3.2. Characteristics of Power Produced by LPG Engines

The dynamic performance of LPG engine power with AICS is presented in Figure 5, showing the relationship between engine speed (4000–6500 rpm) and engine power (Hp) with and without AICS. Both curves showed a nonlinear trend characterized by an increase in power reaching a peak point, followed by a decline at higher engine speeds. Under the condition with AICS (solid line), the engine power increased significantly from approximately 4.0 Hp at 4000 rpm to a peak of 6.0 Hp within the range of 4900–5100 rpm. Furthermore, minor fluctuations occurred while maintaining relatively high power output up to approximately 5800 rpm, before gradually decreasing to 4.0 Hp at 6500 rpm. In comparison, the power increased from approximately 2.0 Hp at 4000 rpm to a maximum of around 5.3 Hp within the range of 5200–5400 rpm without AICS (dashed line), followed by a consistent decline to 3.7 Hp at 6500 rpm.

The most significant difference occurred within the 4800–5200 rpm range, where the power difference reached approximately 0.7–1.0 Hp (13–18%) compared to the condition without AICS. This area (shown in Figure 4) indicated that the implementation of AICS produced higher intake air density, thereby improving the power and volumetric efficiency of LPG engine. However, at engine speeds above 5800 rpm, both systems showed a similar declining trend in power output. Quantitatively, the area under the curve (representing the total engine work within a certain rpm range) showed that the configuration equipped with AICS provided superior overall performance.

In addition to evaluating the engine power characteristics, the implementation of AICS was assessed through statistical analysis. The engine power data obtained before and after the implementation of AICS were analyzed using IBM SPSS Statistics with the non-parametric Wilcoxon Signed-Rank Test, as shown in Appendix 2. The analysis yielded a significance value (p-value) of 0.025, which was lower than 0.05. Therefore, the null hypothesis (H_0) was rejected, while the alternative hypothesis (H_1) was accepted. These results indicated that the implementation of AICS had a statistically significant effect on improving engine power.

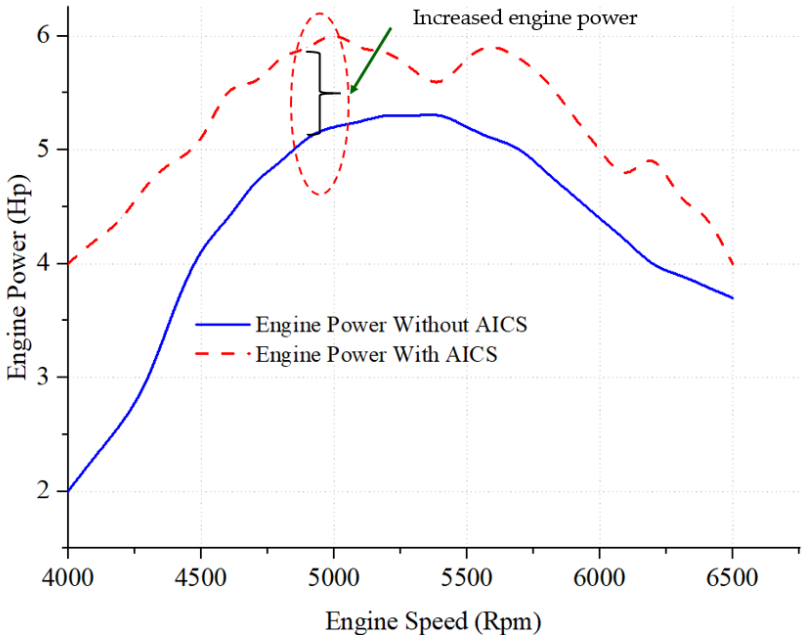

Fig. 5. Increased engine power when the ambient air temperature is hot

3.3. Characteristics of Torque Produced by LPG Engines

LPG engine torque variation is shown in Figure 6 as a function of engine speed (4000–6500 rpm) with and without AICS. The torque curve of LPG engine showed a typical internal combustion engine behavior, where torque increased to a peak at medium engine speeds. This was followed by a gradual decrease at higher speeds due to limitations in cylinder filling and combustion dynamics. Under AICS configuration (solid line), the torque increased from approximately 7.0 Nm at 4000 rpm to a peak of about 8.4–8.5 Nm within the range of 4700–4900 rpm. Meanwhile, without AICS (dashed line), the maximum torque reached only approximately 8.1–8.2 Nm within the same speed range. Therefore, an increase in peak torque of approximately 0.3 Nm was observed, corresponding to a relative improvement of 3.5–4%.

The most significant difference was observed in the 4500–5000 rpm range, where the torque difference was in the range of 0.2–0.4 Nm. The range represented the engine's optimal operating area, having a direct impact on acceleration performance and overall engine efficiency. This phenomenon can be attributed to the ability of AICS to increase the volumetric efficiency of air entering LPG engine. Therefore, the combustion process becomes more effective and generates higher combustion pressure. At engine speeds above 5200 rpm, both configurations showed a relatively sharp decline in torque. However, AICS maintained a relative advantage of approximately 3–6% compared to the non-controlled system at 6000 rpm. The smaller difference suggested a reduced influence of intake-air cooling due to other limiting factors, such as low combustion time and increased mechanical losses. From a quantitative perspective, the integration of the area under the torque curve indicated that AICS provided a higher total work output in the medium operating range, which represented the dominant condition in real driving scenarios. This has positive implications for energy efficiency and the potential reduction in fuel consumption.

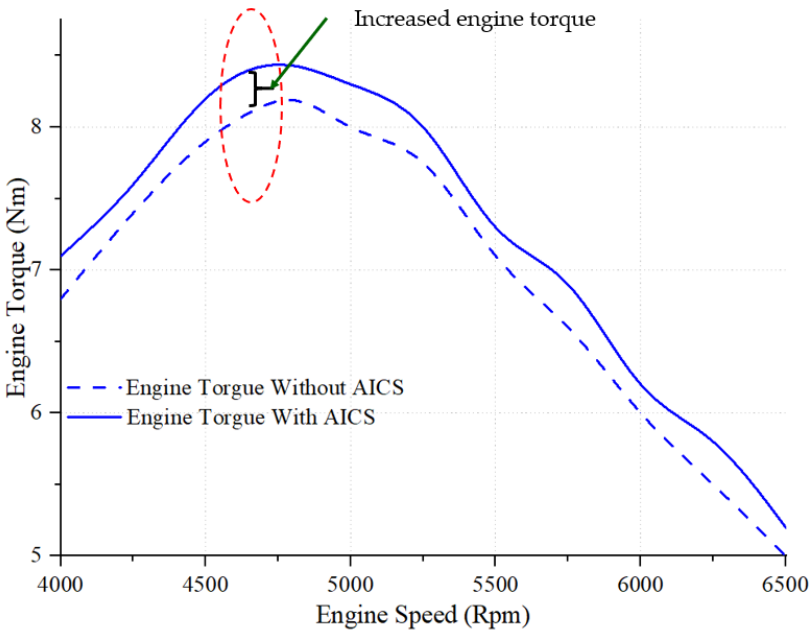

Fig. 6. Increased engine torque when the ambient air temperature is hot

In addition to evaluating the engine torque characteristics, the implementation of AICS was assessed using statistical analysis. The engine torque data obtained before and after the implementation of AICS were analyzed using IBM SPSS Statistics, following the same statistical procedure applied to the engine power analysis, as presented in Appendix 3. The analysis obtained a significance value (p-value) of 0.036, which was lower than the significance level of 0.05. Therefore, the null hypothesis (H_0) was rejected, while the alternative hypothesis (H_1) was accepted. These results indicate that the implementation of AICS has a statistically significant effect on improving engine torque.

3.4. AFR Dynamics, LPG Flow and Air Flow

The change in AFR of LPG engine shows the dynamics of the air-fuel mixture ratio against time during the test interval of 0–100 seconds tested at high speed, as shown in Figure 7. At the initial stage of operation at lower engine speed, AFR is approximately 14.5. However, when the engine operates at higher speed, AFR decreases slightly, ranging from approximately 14.1 to 14.3, with an average value close to 14.2. The maximum deviation was ±0.1–0.15, indicating a high level of stability in the air–fuel mixture. These fluctuations showed a quasi-periodic behavior, associated with the fuel control system's dynamic response to minor variations in engine load or thermal conditions.

From a combustion performance perspective, AFR around 14.2 suggested operation under slightly richer-than-stoichiometric conditions for LPG combustion. This condition is typically used to enhance combustion stability, prevent knocking, and improve power output, particularly under medium-to-high load operation. However, the observed small deviations indicate that the control system is capable of maintaining a balance between power demand and fuel efficiency without introducing significant fluctuations that can degrade engine performance.

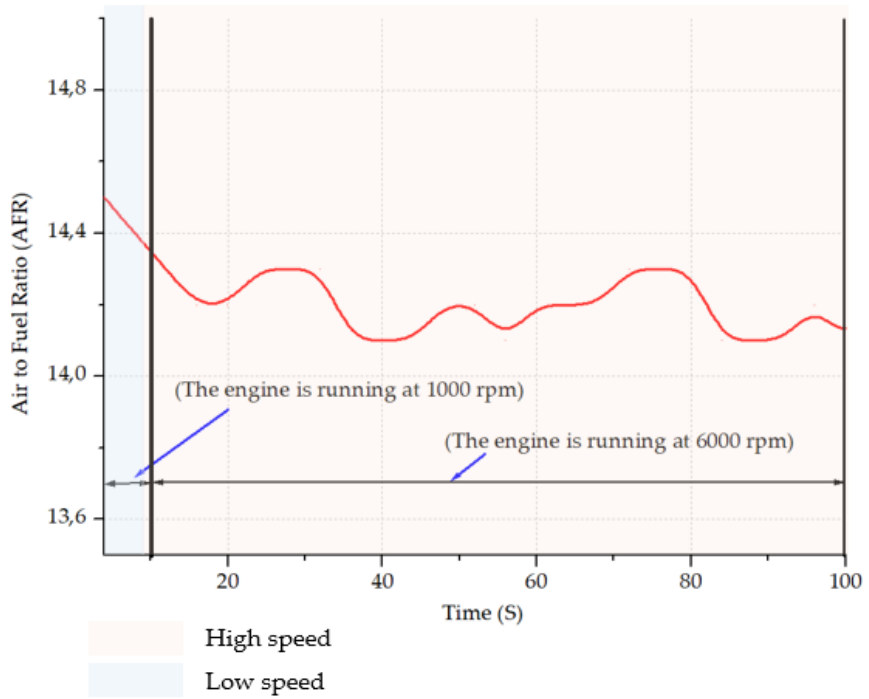

Fig. 7. Changes to the AFR of the LPG engine

The flow changes in LPG engine are represented in Figure 8, showing the characteristics of LPG flow versus time at low to high engine speeds. In the initial testing phase, when the engine was at a low speed of 1000 rpm, LPG flow was approximately 3.0 g/s.s. This value remained relatively stable until approximately the 8th second, before a significant increase occurred as the engine speed was raised toward 6000 rpm. The increase in engine speed led to a higher combustion energy demand, causing a corresponding rapid rise in LPG fuel supply. Following the speed transition, LPG mass flow rate increased sharply from approximately 3.0 g/s to 5.0 g/s within a relatively short time span of 10–20 s. The rapid response indicated that the fuel supply system is capable of quickly adapting to changes in engine load conditions. Quantitatively, this represented an increase of approximately 66–70% compared to the initial condition. The phenomenon indicated a strong positive correlation between engine speed and LPG fuel consumption. Under steady-state conditions after the 20th second, LPG flow rate stabilized at approximately 5.0–5.1 g/s, with relatively small fluctuations. The minor variations are attributed to combustion dynamics, fluctuations in LPG supply pressure, and the fuel regulator's response to small variations in engine operating conditions. However, the low amplitude of the fluctuations shows that the fuel system maintains good operational stability at high engine speed.

The air flow dynamics in the intercooler over the vehicle test time are presented in Figure 9. In the initial stage of the experiment, when the engine operates at approximately 1000 rpm, the air mass flow rate ranges between 43–48 g/s. This value indicates that the air requirement for combustion at low engine speed remains relatively small, as the intake air volume follows the low intake stroke frequency of the engine. After the engine speed rose to 6000 rpm, the air flow rate increased significantly within a short period. The air mass flow rate increased significantly to 71–73 g/s within a time interval of 10–20 s. Quantitatively, this represented an increase of approximately 50% compared to the initial condition.

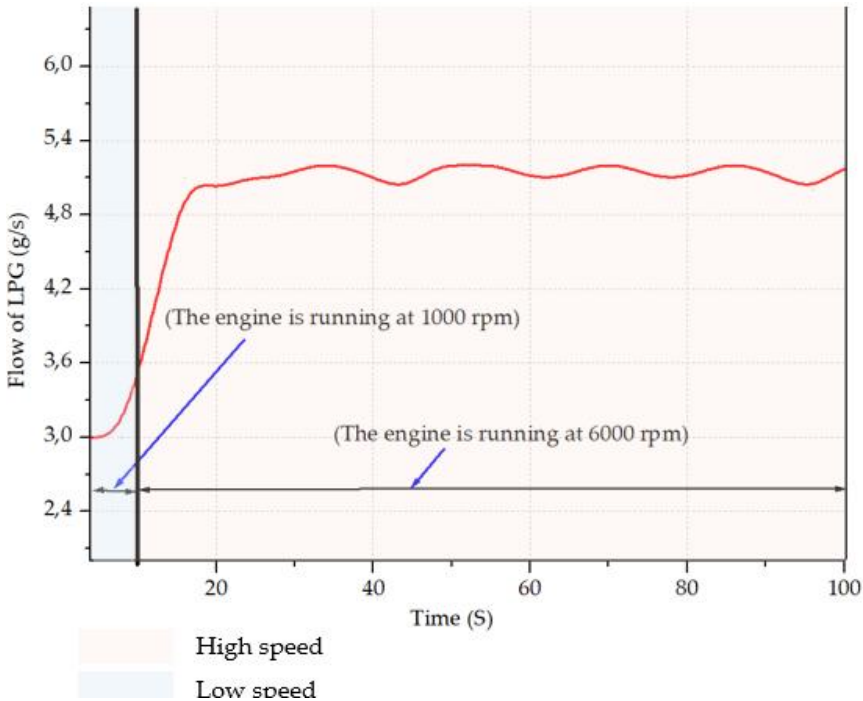

Figure 8. LPG flow dynamics

The increase indicated that higher engine speeds require a greater amount of combustion air to maintain an optimal AFR during the combustion process. The rapid rise during the transition phase suggested that the intake system showed good dynamic responsiveness to changes in engine load. The air intake system was capable of rapidly increasing airflow as the throttle valve opening and engine speed increased. This behavior played an important role in maintaining combustion stability, particularly at high-speed operation where a larger oxygen supply is required. Under steady-state conditions after the 20th second, the air flow rate stabilized at approximately 71–73 g/s with slight fluctuations in the test. The variation was influenced by flow turbulence in the intake manifold, changes in intake air pressure, and combustion dynamics within the cylinder. However, the low amplitude of these fluctuations indicated that the air supply system maintained good operational stability under high engine speed conditions.

Changes in the Standard Deviation (SD) and Margin Of Error (MoE) values calculated using Equations (7) and (8) for the LPG engine's AFR, LPG flow dynamics, and air flow dynamics—are presented in Table 3.

Table 3. Changes in the LPG engine AFR, LPG flow dynamics, and air flow dynamics

No.	Description	Average	SD	MoE
1.	AFR of the LPG engine	14,19	0,08	0,0001
2.	LPG flow dynamics	5,14	0,071	0,0001
3.	Air flow dynamics	72,83	0,912	0,0017

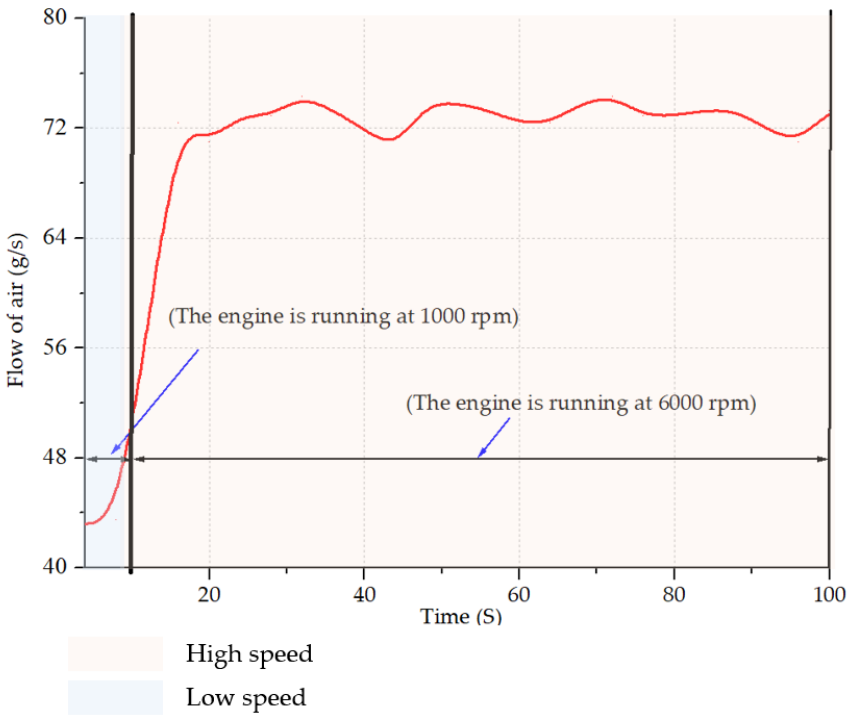

Fig. 9. Air flow dynamics

3.5. Dynamics of Air Temperature Entering the Engine

The changes in air entering LPG engine are shown in Figure 10, as indicated by a continuous blue line, while the air exiting is represented by a red dashed line. The intake air dynamics in LPG engine were categorized into three operating conditions. In the first condition, the engine operated at a low speed of approximately 1000 rpm, and the air entering the intercooler was heated using a heater. During this phase, the inlet air temperature was approximately 28°C at the 1st second and increased to about 40°C by the 9th second. In the second condition, the engine operated at a high speed of approximately 6000 rpm starting at the 91st second. At the 100th second, the inlet air temperature decreased to approximately 31°C. Meanwhile, the air exiting the intercooler was approximately 28°C at the 1st second, which was identical to the inlet air temperature. At the 9th second, the outlet air temperature increased to 36°C, and by the 100th second it decreased again to approximately 28°C.

Under the third condition, AICS started operating when the ambient air temperature exceeded 30°C to cool the intake air supplied to LPG engine. The cooling performance was indicated by the temperature difference between the inlet and outlet air of the intercooler. At the 9th second, the inlet air temperature was approximately 40°C, while the outlet had 36°C, causing a temperature difference (ΔT) of 4°C. At the 100th second, the inlet air temperature was 31°C, while the outlet air had 28°C, corresponding to a ΔT of 3°C. These results indicated that AICS could reduce the intake air temperature by approximately 3–4°C. However, the cooling performance decreases at high engine speeds due to three main factors. First, engine operation at high speed generated significant heat, which was conducted toward the intercooler and affected its cooling effectiveness. Second, the intercooler was installed extremely close to the engine, increasing heat transfer from the engine to the intercooler. Third, the intercooler was connected to the engine using metal piping. The conduction phenomenon through both the installation proximity and metal piping significantly affected intercooler performance and reduced cooling capability under high-speed operating conditions.

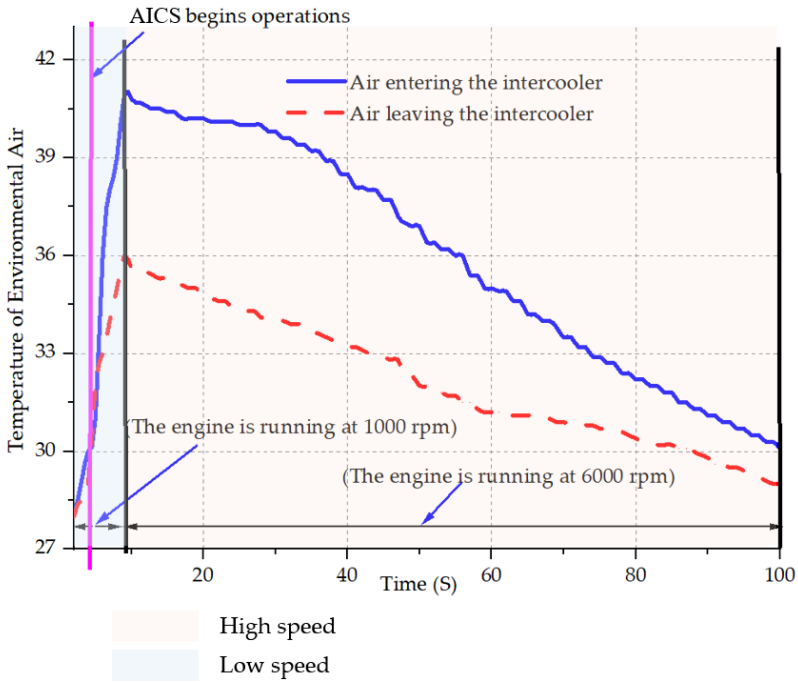

Fig. 10. Changes in the air entering the LPG engine

3.6. LPG Temperature Changes in the Intercooler

The dynamics of LPG entering the engine are presented in Figure 11 and are categorized into three operating conditions. LPG entering the intercooler is indicated by a red dashed line, while LPG exiting the intercooler is represented by a continuous blue line. In the first condition, the engine operated at a low speed of approximately 1000 rpm. LPG temperature reached the lowest value of 18°C, followed by a gradual increase to approximately 19°C. This increase indicated the initial response of the system as LPG flow started interacting thermally with the surrounding environment and intercooler components. At this stage, the temperature difference between inlet and outlet remained relatively small (<1°C), indicating that heat transfer had not significantly developed.

In the second condition, AICS started operating, leading to a more stable and directed temperature increase. At approximately 10 s, LPG inlet temperature increased to 18.6°C, while the outlet value reached 18.9°C. This variation suggested that the process was dominated by convective heat transfer, where thermal energy was transferred from the surrounding air to LPG through heat exchanger wall. In the third condition, the engine operated at a high speed of approximately 6000 rpm, and the temperature increase became more gradual but consistent. LPG inlet temperature increased to approximately 22.8°C, while the outlet value reached 23.7°C at the end of the test ($t \approx 100$ s). The temperature difference between inlet and outlet (ΔT) remained relatively stable in the range of 0.5–1°C throughout this condition. Quantitatively, the total increase in LPG temperature was approximately 4–5°C from the initial to the final condition. The increase indicated that LPG acted as an effective heat-absorbing medium within the intercooler. This suggested that thermal energy from the air was successfully transferred to LPG, contributing to the reduction in air temperature, as presented in Figure 11.

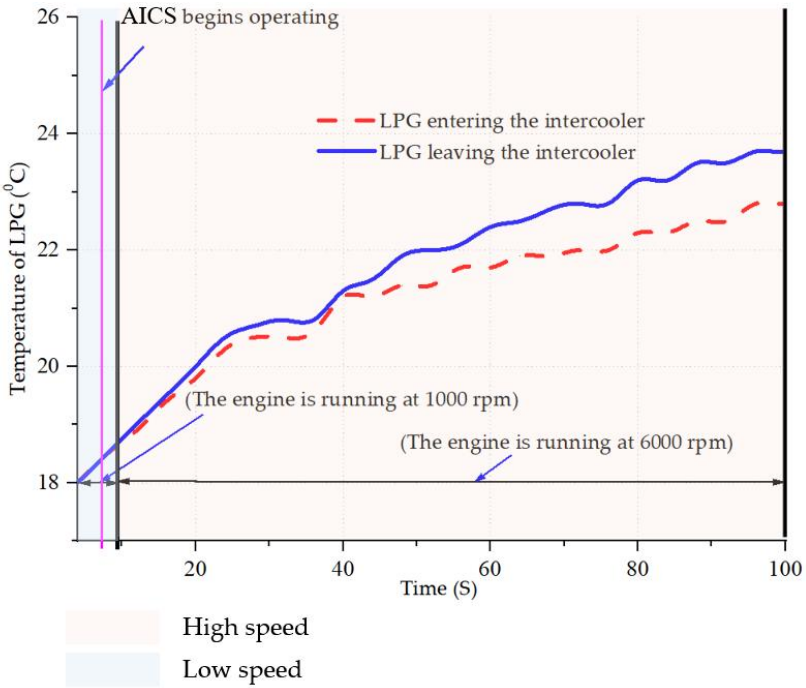

Fig. 11. Changes in the temperature of LPG entering the LPG engine

3.7. Air Heat Transfer with AICS

The characteristics of heat transfer in air, calculated using Equation (6), are presented in Figure 12. Based on observation, the air heat transfer characteristics showed significant variations with engine operating time and speed conditions. In the initial phase of the experiment, when AICS started operating, the air heat transfer rate increased rapidly from near 0 W to 4.8 W. This increase indicated that the activation process of the cooling system influenced by AICS caused a rise in intensity of air flow and temperature changes through the intercooler. The condition indicated a significant increase in heat transfer, which was strongly influenced by the engine speed and the operation of AICS.

After the system was fully activated, the air heat transfer continued to increase gradually and reached a maximum value of approximately 5.5–5.6 W within the time interval of 25–35 s. This phenomenon indicated that at low engine speed (approximately 1000 rpm), the system maintained relatively high heat transfer effectiveness. The stability of heat transfer value during this period indicated that the temperature difference between heat medium and the air remained sufficiently large to maintain the driving force for thermal transfer.

As the operation time and engine speed increased toward 6000 rpm, the air heat transfer rate gradually decreased. This condition occurred because the intercooler was installed directly above the engine, allowing heat propagation from the engine to the intercooler, which affected the air heat transfer performance. In the 40–70 s interval, heat transfer rate decreased from approximately 5 W to 2.5 W. However, during the 10–40 s interval, heat transfer rate remained in an optimal condition for heat removal from the intercooler, as LPG self-refrigeration process controlled by AICS was able to effectively cool the incoming air to the engine.

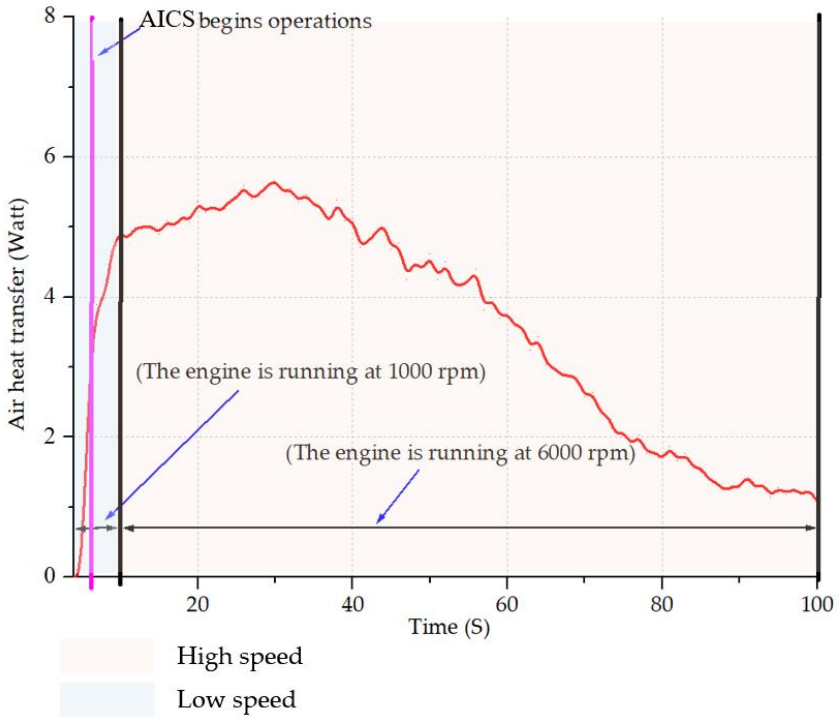

Fig. 12. Air heat transfer

3.8. Heat Transfer Changes with AICS

Heat transfer dynamics of LPG in the intercooler calculated based on Equation (4) are presented in Figure 13. Based on this graph, heat transfer characteristics of LPG showed a significant change after IHCS started operation. In the initial phase of the experiment, before 10 s, LPG heat transfer rate remained close to 0 W. This condition indicated that heat exchange between LPG and the thermal medium remained suboptimal because the system was close to effective operating conditions. At this stage, both the temperature and mass flow rate of LPG were still relatively low, leading to limited thermal energy that could be absorbed by LPG. When AICS became active at approximately 10–12 s, a sharp increase in heat transfer occurred, rising from 0 W to more than 125 W. This significant increase indicated a significant enhancement in evaporation intensity and heat absorption by LPG due to the large temperature difference between heat source and LPG fluid. The phenomenon showed that LPG has a very high capacity for heat absorption during both phase change and sensible heating processes.

After reaching operating conditions, LPG heat transfer rate remained relatively stable in the range of 123–128 W until the end of the experiment at 100 s. This stability indicated that heat transfer system reached a quasi-steady-state condition, where the thermal energy absorbed by LPG remained approximately constant. Minor fluctuations in the curve suggest variations in LPG mass flow rate, transient temperature changes, and engine combustion dynamics during the transition from 1000 rpm to 6000 rpm. However, the relatively small amplitude of these fluctuations indicated good thermal stability of the system.

Compared with air-side heat transfer, LPG heat transfer rate showed a significantly higher value, reaching 125 W, while the air heat transfer rate was only in the range of 5–6 W. This difference indicated that LPG acted as the dominant heat-absorbing medium in the system used to cool the intake air. The high heat transfer capacity of LPG was strongly influenced by thermophysical properties, particularly the large latent heat of vaporization, which enabled absorption of a substantial amount of thermal energy during phase change processes.

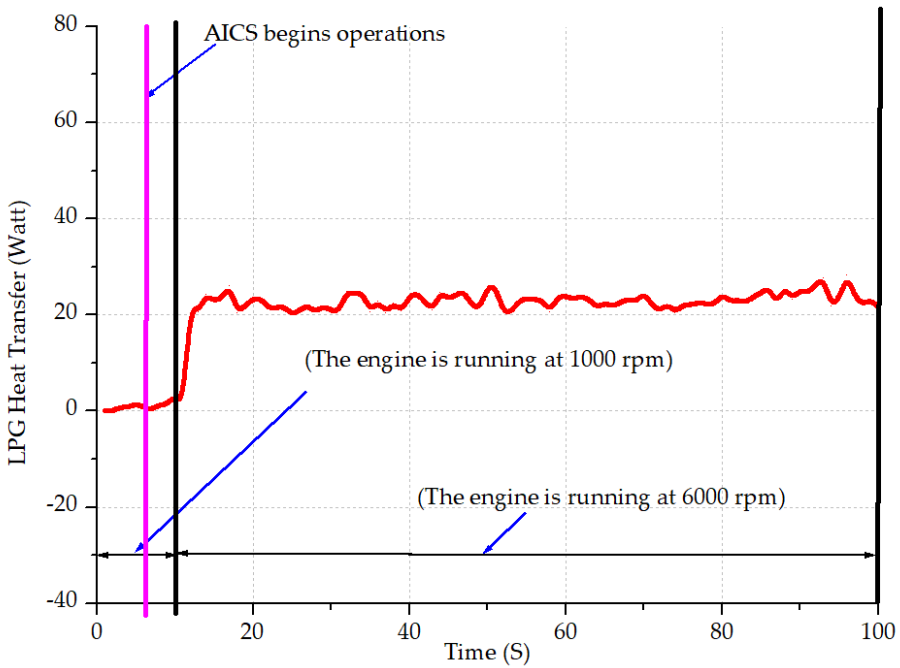

Fig. 13. Heat transfer characteristics of LPG

Changes in the Standard Deviation (SD) and Margin Of Error (MoE) values calculated using Equations (7) and (8) for temperature differential of the air entering the engine, temperature differential of the LPG entering the engine, air heat transfer and Heat transfer of LPG are presented in Table 4.

Table 4. Changes in the temperature differential of the air entering the engine, temperature differential of the LPG entering the engine, air heat transfer and Heat transfer of LPG.

No.	Description	Average	SD	MoE
1.	Temperature differential of the air entering the engine	3,55	1,67	0,0031
2	Temperature differential of the LPG entering the engine	0,55	0,35	0,0006
3.	Air heat transfer	3,43	1,61	0,0029
4..	Heat transfer of LPG	22,95	1,72	0,0031

4. Discussion

The design of AICS for LPG-fueled engines was evaluated based on five main parameters, namely exhaust emissions, engine power, engine torque, air heat transfer, and LPG heat transfer. The evaluation results showed that the developed system was capable of improving engine performance while simultaneously supporting environmental sustainability. The initial evaluation focused on exhaust emission characteristics, with experimental results showing that AICS significantly reduced emissions from LPG-fueled engines, improving their environmental performance. A substantial reduction was observed in HC and CO emissions, both of which are harmful pollutants to the environment. This reduction occurred because the cooled intake air lowered the combustion chamber temperature, leading to a more controlled combustion process. The lower combustion temperature contributed to the reduction of hazardous exhaust gases.

The second evaluation examined changes in engine power. Based on dynotest measurements, AICS was proven to enhance the power output of LPG engine under high ambient temperature conditions. The engine power increased by approximately 0.7–1.0 HP, equivalent to 13–18%, within the engine speed range of 4800–5200 rpm. Under high ambient temperatures, air molecules become more dispersed, reducing air density and consequently decreasing the volumetric efficiency of the engine. A reduction in engine volumetric efficiency negatively impacts suboptimal combustion quality and decreases engine power. AICS cools the incoming air through LPG phase-change self-refrigeration effect, thereby increasing engine power under hot ambient conditions.

The third evaluation investigated engine torque characteristics. The results showed that AICS was capable of optimally increasing engine torque within the engine speed range of 4000–5000 rpm, with a rise of approximately 0.2–0.4 Nm. This engine speed range represents the optimal operating condition of the engine. Therefore, the torque improvement has direct implications for engine performance and operational efficiency. The increase in torque and power of LPG engine occurs due to the cooling of the incoming air, specifically in hot ambient temperature conditions. These results are consistent with previous studies indicating that engine performance is strongly influenced by volumetric efficiency (Hofmann, 2017). Consequently, AICS was proven to minimize the loss of engine power and torque during operation in hot environmental conditions.

The fourth evaluation analyzed heat transfer of intake air in the intercooler system. The results showed that AICS increased the air heat transfer rate optimally within the time interval of 25–35 s, reaching values of approximately 5.5–5.6 Watts. The optimal condition was achieved due to the self-refrigeration effect of LPG controlled by AICS. After this period, heat transfer rate gradually decreased because the intercooler was installed extremely close to the engine block, resulting in heat conduction from the engine to the intercooler. This heat propagation reduced the cooling effectiveness of the intake air. Therefore, future system development should consider repositioning the intercooler farther away from the engine block to minimize conductive heat transfer effects.

The fifth evaluation focused on LPG heat transfer in the intercooler. The results showed that AICS produced a relatively stable LPG heat transfer rate in the range of 123–128 Watts until the end of the 100-second testing period. This stability indicated that heat transfer system had reached a near steady-state thermal condition, allowing the intake air cooling process to operate consistently. The high heat transfer capacity of LPG effectively cooled the air passing

through the intercooler. However, the cooling process was only effective under high ambient temperature conditions. When applied in cold environmental conditions, excessive cooling could negatively affect the mixing process between LPG and air, thereby reducing combustion quality. Therefore, AICS was designed to regulate the cooling process, activating only under high ambient temperatures and automatically deactivating under low-temperature conditions.

The results regarding the use of LPG/propane mixture as a cooling medium through the self-refrigeration effect phenomenon are supported by Setiyo *et al.*, (2017a); Shady, Ahmed, and Sleiti, (2024); Setiyo *et al.*, (2017b), which showed the strong potential for the development of alternative cooling systems. Waluyo *et al.*, (2022) used the cooling effect due to LPG evaporation applied to the vehicle cabin cooling system. In comparison, this study showed that the self-refrigeration effect of LPG directly affected engine performance, as evidenced by reduced emissions and increased engine power and torque. The results confirmed that the developed AICS technology improved the performance of LPG-fueled engines, thereby contributing to the advancement of more environmentally friendly automotive technologies.

4.1. Conclusion

In conclusion, this study shows that the proposed AICS design effectively addresses the performance issues encountered in LPG-fueled engines, particularly the power loss that occurs under high ambient temperature conditions. The system was evaluated based on five key aspects: engine power, engine torque, air heat transfer, exhaust emissions, and LPG heat transfer. The AICS operates effectively by utilizing the self-cooling effect of LPG, boosting engine power by approximately 0.7–1.0 hp (13–18%) within the 4800–5200 rpm range. Additionally, it increases torque by about 0.2–0.4 Nm between 4000 and 5000 rpm, especially during high ambient temperature operations. The AICS also contributes to reduced exhaust emissions, as observed during idle speed testing; the mechanism lowers HC and CO emissions by cooling the intake air, thereby reducing in-cylinder temperatures and suppressing the formation of harmful exhaust gases.

From a thermal perspective, AICS enhances air-side heat transfer in the intercooler, reaching an optimal value of approximately 5.5–5.6 W within the 25–35 s interval, while maintaining stable LPG heat transfer in the range of 20–26 W until the end of the experiment. This thermal stability indicates that the system has achieved an effective operating condition for cooling the intake air. The reduction in intake air temperature also shifts the air-fuel mixture closer to stoichiometry (with the AFR rising from 14.75 to 14.85) and increases exhaust oxygen levels from 4.5% to 6.3%. However, the cooling effectiveness is influenced by the intercooler proximity to the engine block, which allows heat propagation from the engine and reduces the overall cooling performance. Therefore, further development is required in terms of intercooler design and placement to achieve more optimal system performance.

4.2. Acknowledgment

The authors are grateful to the Directorate of Research and Community Service (DPPM), Ministry of Education, Culture, Research, and Technology (Kemendikbudristek), as well as the Research and Community Service Institute of Universitas Muhammadiyah Magelang for their support in facilitating and funding this study.

Nomenclature:

$0{,}5(propane + butane)_1$	- LPG mixture in the output line
$0{,}5\ (propane + butane)_2$	- LPG mixture in the input line
AFR	- Air-LPG Mixture
$\dot{m_{air}}$	- Flow of air (g/s)
$\dot{m_{LPG}}$	- Flow of LPG (g/s)
m_1	- Initial LPG mass
m_2	- LPG mass at the end of the period (S)
q_{LPG}	- Heat transfer of LPG (Watt)
Δh	- LPG enthalpy difference
q_{air}	- Heat transfer of air (Watt)
CP_{air}	- Specific heat capacity of air (J.kg-1.C-1)
ΔT_{air}	- Difference in air temperature in units (°C)
SD	- Standard Deviation
MoE	- Margin of Error
Z	- Confidence level
n	- The number of data points or samples

References

1. Amer, A. A., Gad, H. M., Ibrahim, I. A., Abdel-Mageed, S. I., & Farag, T. M. (2015). Experimental Study of LPG Diffusion Flame at Elevated Preheated Air Temperatures. *International Journal of Mechanical and Mechatronics Engineering*, *9*(8), 1499–1506. https://doi.org/doi.org/10.5281/zenodo.1108072
2. Anantama, H., Achmad Fuad, E., Waluyo, B., & Saifudin, S. (2023). Improved Engine Performance Using Ozone Generator. *Borobudur Engineering Review*, *3*(2), 17–25. https://doi.org/10.31603/benr.9083
3. Bergougui, B. (2024). Moving toward environmental mitigation in Algeria: Asymmetric impact of fossil fuel energy, renewable energy and technological innovation on CO2 emissions. *Energy Strategy Reviews*, *51*(December 2023), 101281. https://doi.org/10.1016/j.esr.2023.101281
4. Churchill, R., Sharma, M., Olsen, D., & Windom, B. (2025). Suitability of DME/LPG blends for SI engines: Reactivity and spray characterization through research and motor octane number measurements coupled with optical imaging techniques. *Fuel*, *402*, 135976. https://doi.org/10.1016/j.fuel.2025.135976
5. Cipollone, R., Di Battista, D., & Vittorini, D. (2017). Experimental assessment of engine charge air cooling by a refrigeration unit. *Energy Procedia*, *126*, 1067–1074. https://doi.org/10.1016/j.egypro.2017.08.226
6. Dafis, A., Rottengruber, H., & Rabe, B. (2026). Investigation of combustion and performance limits of liquid LPG direct injection in a single-cylinder research engine. *Automotive and Engine Technology*, *11*(11), 1–14. https://doi.org/10.1007/s41104-026-00173-1
7. Hofmann, F. (2017). *Converting Vehicles to Propane Autogas Part 1 : Installing Fuel Tanks and Fuel Lines* (Edisi ke-1). Propane exceptional energy.
8. Kim, J. K., Lee, W.-J., Ahn, E., & Choi, J.-H. (2025). Experimental and numerical studies on performance investigation of a diesel engine converted to run on LPG. *Energy Conversion and Management*, *321*, 119091. https://doi.org/10.1016/j.enconman.2024.119091
9. Kozyra, J., Łukasik, Z., Kuśmińska-Fijałkowska, A., Folęga, P., & Janota, A. (2025). Standards And Requirements Concerning Reduction of Co2 Emission for New Passenger Cars. *Archives of Transport*, *74*(2), 7–22. https://doi.org/10.61089/aot2025.whr7qq76
10. Mahlangeni, N., Kapwata, T., Webster, C., Howlett-Downing, C., & Wright, C. Y. (2025). Exposure to air pollution from coal-fired power plants and impacts on human health: a scoping review. *Reviews on Environmental Health*, *40*(4), 834–855. https://doi.org/10.1515/reveh-2024-0173
11. Masi, M., & Gobbato, P. (2012). Measure of the volumetric efficiency and evaporator device performance for a liquefied petroleum gas spark ignition engine. *Energy Conversion and Management*, *60*, 18–27. https://doi.org/10.1016/j.enconman.2011.11.030
12. Matthujak, A., Wichangarm, M., Sriveerakul, T., Sucharitpwatskul, S., & Phongthanapanich, S. (2021). Numerical investigation on the influences of swirling flow to thermal efficiency enhancement of an LPG-energy saving burner. *Case Studies in Thermal Engineering*, *28*(September), 101466. https://doi.org/10.1016/j.csite.2021.101466
13. Mohsen, M. J., Al-Dawody, M. F., Jamshed, W., El Din, S. M., Sirelkhtam Elmki Abdalla, N., Abd-Elmonem, A., Iqbal, A., & Hussain Shah, H. (2023). Experimental and numerical study of using of LPG on characteristics of dual fuel diesel engine under variable compression ratio. *Arabian Journal of Chemistry*, *16*(8), 104899. https://doi.org/10.1016/j.arabjc.2023.104899
14. Muji Setiyo, Sudjito Soeparman , Nurkholis Hamidi, S. W. (2017). Cooling effect characteristics of a ½ cycle refrigeration system on an LPG fuel system. *International Journal of Refrigeration*, *82*, 227–237. https://doi.org/https://doi.org/10.1016/j.ijrefrig.2017.06.009
15. Munahar, S., Rusdjijati, R., Hanafi, M., & Waryono, A. (2026). Case Studies in Thermal Engineering Assessment of Intake Air Temperature Control (IATC) by utilizing the self-cooling effect in Liquefied Petroleum Gas (LPG) engines. *Case Studies in Thermal Engineering*, *82*(April), 108036. https://doi.org/10.1016/j.csite.2026.108036

16. Munahar, S., Setiyo, M., Saudi, M. M., Ahmad, A., Dhimas R, A. A., & Hardiansyah, M. (2024). Assessment of comfort index (CI) based on vibration characteristics in CNG control system development. *Results in Engineering*, *21*(January), 101840. https://doi.org/10.1016/j.rineng.2024.101840
17. Novella, R., Dolz, V., Martín, J., & Royo-Pascual, L. (2017). Thermodynamic analysis of an absorption refrigeration system used to cool down the intake air in an Internal Combustion Engine. *Applied Thermal Engineering*, *111*, 257–270. https://doi.org/10.1016/j.applthermaleng.2016.09.084
18. Ohunakin, O. S., Adelekan, D. S., Babarinde, T. O., Leramo, R. O., Abam, F. I., & Diarra, C. D. (2017). Experimental investigation of TiO2-, SiO2- and Al2O3-lubricants for a domestic refrigerator system using LPG as working fluid. *Applied Thermal Engineering*, *127*(2017), 1469–1477. https://doi.org/10.1016/j.applthermaleng.2017.08.153
19. Park, J., & Sungwook Park. (2025). Development of CO2 and NOx emission factors for heavy-duty vehicles based on engine dynamometer and real-world emission tests. *Energy*, *339*, 139129. https://doi.org/10.1016/j.energy.2025.139129
20. Salamanca, C. L. M. A., Macabinlar, K. D. A., Apus, S. M. S., Geraldez, C. L. M. G., & Pabilona, L. L. (2024). An experimental study of liquefied petroleum gas refrigeration system. *Palawan Scientist*, *16*(2), 71–81. https://doi.org/10.69721/TPS.J.2024.16.2.07
21. Salman, A. M., Ibrahim, I. A., Gad, H. M., & Farag, T. M. (2020). Effects of Air Temperature on Combustion Characteristics of LPG Diffusion Flame. *Materials Science Forum*, *1008*, 128–138. https://doi.org/10.4028/www.scientific.net/MSF.1008.128
22. Setiyo, M., Condro Purnomo, B., Waluyo, B., Munahar, S., Latifur Rochman, M., Rahman Saleh, A., Desy Fatmaryanti, S., & David Samuel, O. (2022). Cooling power characteristics of half-cycle refrigeration system in LPG fuelled vehicles by auxiliary chiller as heat exchanger. *Thermal Science and Engineering Progress*, *27*(October 2021). https://doi.org/10.1016/j.tsep.2021.101145
23. Setiyo, M., Syaka, D. R. B., Waluyo, B., Hamidi, N., & Kiono, B. F. T. (2017). Cooling effect potential from liquefied petroleum gas flow in the fuel line of vehicle. *International Journal of Automotive and Mechanical Engineering*, *14*(4), 4704–4714. https://doi.org/10.15282/ijame.14.4.2017.9.0370
24. Setiyo, M., Waluyo, B., Husni, M., & Karmiadji, D. W. (2016). Characteristics of 1500 CC LPG fueled engine at various of mixer venturi area applied on Tesla A-100 LPG vaporizer. *Jurnal Teknologi*, *78*(10), 43–49. https://doi.org/10.11113/jt.v78.7661
25. Shady, R., Ahmed, S. F., & Sleiti, A. K. (2024). Operation optimization of propane pre-cooled mixed refrigerant LNG Process: A novel integration of knowledge-based and constrained Bayesian optimization approaches. *Chemical Engineering Science*, *300*, 120560. https://doi.org/10.1016/j.ces.2024.120560
26. Simsek, S., & Uslu, S. (2024). Evaluation of the Possible Effects of Varying the Volumetric Ratio of Lpg on the Spark Ignition Engine's Performance, Emissions, and Combustion. *International Journal of Automotive Science and Technology*, *8*(3), 273–278. https://doi.org/10.30939/ijastech..1491371
27. Talib Hashem, G., Al-Dawody, M. F., & Sarris, I. E. (2023). The characteristics of gasoline engines with the use of LPG: An experimental and numerical study. *International Journal of Thermofluids*, *18*(March 2023), 100316. https://doi.org/10.1016/j.ijft.2023.100316
28. Usman, M., Farooq, M., Naqvi, M., Saleem, M. W., Hussain, J., Naqvi, S. R., Jahangir, S., Jazim Usama, H. M., Idrees, S., & Anukam, A. (2020). Use of gasoline, LPG and LPG-HHO blend in SI engine: A comparative performance for emission control and sustainable environment. *Processes*, *8*(1), 1–15. https://doi.org/10.3390/pr8010074
29. Vishnuram, P., Alagarsamy, S., Bajaj, M., Alqahtani, M., & Khalid, M. (2025). A critical review on alternative fuels for road transportation: Pollution mitigation, environment and economic perspective. *Energy Strategy Reviews*, *61*(March), 101894. https://doi.org/10.1016/j.esr.2025.101894
30. Wallbanks, S., Griffiths, B., Thomas, M., Price, O. J., & Sylvester, K. P. (2024). Impact of environmental air pollution on respiratory health and function. *Physiological Reports*, *12*(16), 1–13. https://doi.org/10.14814/phy2.70006

31. Waluyo, B., Setiyo, M., Purnomo, B. C., Rochman, M. L., Habibi, I., Saleh, A. R., Suyitno, Fatmaryanti, S. D., & Kolakoti, A. (2022). Cooling effect characteristic of the novel half-cycle refrigeration system on a liquefied petroleum gas (LPG) fueled vehicle. *Thermal Science and Engineering Progress*, *34*(July 2022). https://doi.org/10.1016/j.tsep.2022.101405
32. Wang, T., Yang, P., Yi, W., Luo, Z., Cheng, F., Ding, X., Kang, X., Feng, Z., & Deng, J. (2022). Effect of obstacle shape on the deflagration characteristics of premixed LPG-air mixtures in a closed tube. *Process Safety and Environmental Protection*, *168*(September), 248–256. https://doi.org/10.1016/j.psep.2022.09.079
33. Xiangyang, W., Yu, L., Xiaoping, L., Fangxi, X., & Beiping, J. (2024). Experimental study on improvement of air-dilution combustion performance of methanol engine by adjusting intake guide flappers, exhaust variable valve timing and split injection. *Energy*, *313*, 133825. https://doi.org/10.1016/j.energy.2024.133825
34. Zhang, Z., Wan, W., & Wencan Zhang, Qin Liu, Rongchao Zhao, Youpeng Chen, Q. Q. (2022). Research of the impacts of in-cylinder steam injection and ignition timing on the performance and NO emission of a LPG engine. *Energy*, *244*, 123193. https://doi.org/https://doi.org/10.1016/j.energy.2022.123193

Appendix 1: Script Programming

```
#include <DHT.h>
#include <Wire.h>
#include <LiquidCrystal_I2C.h>

#define DHTPIN A0       // A0 digital pin 14
#define DHTTYPE DHT11

DHT dht(DHTPIN, DHTTYPE);

// Addres I2C LCD (0x27 / 0x3F / 0x22 request from module )
LiquidCrystal_I2C lcd(0x22, 16, 2);

int relayPin1 = 2;   // Main Solenoid 1
int relayPin2 = 3;   // Main Solenoid 2
int relayPin3 = 4;   // Bypass Solenoid 1
int relayPin4 = 5;   // Bypass Solenoid 2

float temperature = 0;
float humidity = 0;

void setup() {
  pinMode(relayPin1, OUTPUT);
  pinMode(relayPin2, OUTPUT);
  pinMode(relayPin3, OUTPUT);
  pinMode(relayPin4, OUTPUT);

  Serial.begin(9600);
  dht.begin();

  // Inisialisasi LCD
  lcd.init();
  lcd.backlight();
  lcd.clear();
```

```
  lcd.setCursor(0, 0);
  lcd.print("DHT11 Sensor");
  delay(2000);
  lcd.clear();
}

void loop() {
  temperature = dht.readTemperature();
  humidity = dht.readHumidity();

  if (isnan(temperature) || isnan(humidity)) {
    lcd.clear();
    lcd.setCursor(0, 0);
    lcd.print("Error Sensor!");
    Serial.println("Error reading temperature/humidity ");
    delay(2000);
    return;
  }

  // Convert temperature to an integer for binary representation
  int temperatureInt = (int)temperature;

  // --- Serial Monitor ---
  Serial.print("Temperature : ");
  Serial.print(temperature, 2);   // 2 decimal numeric
  Serial.print((char)223);
  Serial.print("C  |  Biner: ");
  Serial.println(temperatureInt, BIN);

  Serial.print("Humidity: ");
  Serial.print(humidity, 2);
  Serial.println("%");

  // --- Show in LCD ---
  lcd.clear();

  // Format temperature as string with 2 decimals
  char buffer[8];
  dtostrf(temperature, 5, 2, buffer); // (value, widh, decimal, buffer)

  lcd.setCursor(0, 0);
  lcd.print("S:");
  lcd.print(buffer);
  lcd.write(223);         // symbol of Degree
  lcd.print("C ");

  lcd.print("B:");
  lcd.print(temperatureInt, BIN);  // show biner

  lcd.setCursor(0, 1);
```

```
  lcd.print("H:");
  lcd.print(humidity, 2);  // show 2  desimal numeric
  lcd.print("%");

  // --- Logic of relay ---
  if (temperature > 30) {
    digitalWrite(relayPin1, HIGH);
    digitalWrite(relayPin2, HIGH);
    digitalWrite(relayPin3, LOW);
    digitalWrite(relayPin4, LOW);
  }
  else if (temperature >= 20 && temperature <= 30) {
    digitalWrite(relayPin1, LOW);
    digitalWrite(relayPin2, HIGH);
    digitalWrite(relayPin3, HIGH);
    digitalWrite(relayPin4, LOW);
  }
  else if (temperature > 0 && temperature <= 20) {
    digitalWrite(relayPin1, LOW);
    digitalWrite(relayPin2, LOW);
    digitalWrite(relayPin3, HIGH);
    digitalWrite(relayPin4, HIGH);
  }

  delay(2000);
}
```

Appendix 2: Engine Power Test Results Analyzed Statistically using Software SPSS

Wilcoxon Signed Ranks Test

Ranks

		N	Mean Rank	Sum of Ranks
Engine power without AICS - Engine power with AICS	Negative Ranks	4[a]	21.75	87.00
	Positive Ranks	22[b]	12.00	264.00
	Ties	0[c]		
	Total	26		

a. Engine power without AICS < Engine power with AICS

b. Engine power without AICS > Engine power with AICS

c. Engine power without AICS = Engine power with AICS

Test Statistics[a]

	Engine power without AICS - Engine power with AICS
Z	-2.249[b]
Asymp. Sig. (2-tailed)	.025

a. Wilcoxon Signed Ranks Test

b. Based on negative ranks.

Appendix 3: Engine Torque Test Results Analyzed Statistically using Software SPSS

Wilcoxon Signed Ranks Test

Ranks

		N	Mean Rank	Sum of Ranks
Engine torque without AICS - Engine torque with AICS	Negative Ranks	21[a]	11.43	240.00
	Positive Ranks	4[b]	21.25	85.00
	Ties	1[c]		
	Total	26		

a. Engine torque without AICS < Engine torque with AICS

b. Engine torque without AICS > Engine torque with AICS

c. Engine torque without AICS = Engine torque with AICS

Test Statistics[a]

	Engine torque without AICS - Engine torque with AICS
Z	-2.097[b]
Asymp. Sig. (2-tailed)	.036

a. Wilcoxon Signed Ranks Test

b. Based on positive ranks.